Computer Assisted Planning and Navigation of Periacetabular Osteotomy with Range of Motion Optimization

Li Liu[1], Timo Ecker[2], Steffen Schumann[1], Klaus Siebenrock[2], Lutz Nolte[1], and Guoyan Zheng[1]

[1] Institute for Surgical Technology and Biomechanics, University of Bern, Switzerland
{li.liu,guoyan.zheng}@istb.unibe.ch
[2] Department of Orthopaedic Surgery, Inselspital, University of Bern, Switzerland

Abstract. Femoroacetabular impingement (FAI) before or after Periacetabular Osteotomy (PAO) is surprisingly frequent and surgeons need to be aware of the risk preoperatively and be able to avoid it intra-operatively. In this paper we present a novel computer assisted planning and navigation system for PAO with impingement analysis and range of motion (ROM) optimization. Our system starts with a fully automatic detection of the acetabular rim, which allows for quantifying the acetabular morphology with parameters such as acetabular version, inclination and femoral head coverage ratio for a computer assisted diagnosis and planning. The planned situation was optimized with impingement simulation by balancing acetabuar coverage with ROM. Intra-operatively navigation was conducted until the optimized planning situation was achieved. Our experimental results demonstrated: 1) The fully automated acetabular rim detection was validated with accuracy 1.1 ± 0.7mm; 2) The optimized PAO planning improved ROM significantly compared to that without ROM optimization; 3) By comparing the pre-operatively planned situation and the intra-operatively achieved situation, sub-degree accuracy was achieved for all directions.

Keywords: Periacetabular osteotomy, surgical planning, range of motion, hip impingement analysis.

1 Introduction

Periacetabular osteotomy (PAO) is an effective approach for surgical treatment of hip dysplasia in young patients. The aim of PAO is to increase acetabular coverage of the femoral head and to reduce contact pressures by realigning the hip joint [1].

It was reported that the most challenging aspect of PAO surgery is to determine the amount of necessary acetabular rotation, and to achieve the optimal alignment intra-operatively [2]. Rodriguez et al. [3] presented an experimental cadaver study for performance of PAOs. They examined how accurately a preoperatively planned angular and rotational acetabular reorientation could be realized. Transfer of this knowledge to the clinical setting has never been performed.

P. Golland et al. (Eds.): MICCAI 2014, Part II, LNCS 8674, pp. 643–650, 2014.

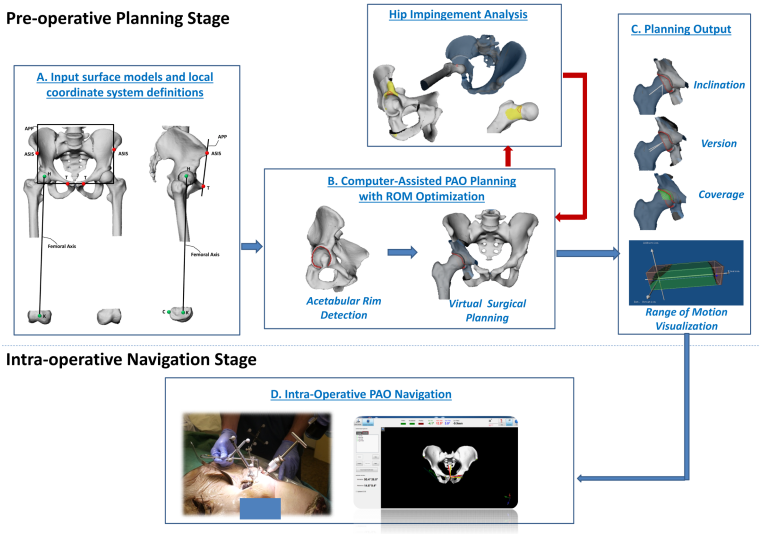

Fig. 1. Schematic view of our computer assisted planning and navigation of PAO with ROM optimization. A. the input surface models and the two local coordinate systems. The pelvic reference is the anterior pelvic plane (APP) defined by both anterior superior iliac spines (ASIS) and the mid-point of the pubic tubercles (T). The femoral axis runs through the hip center (H) and the knee center (K) with the inter-condylar line (C) lying parallel to the APP; B. Computer assisted PAO planning with ROM optimization; C. the pre-operative planning output; D. Intra-operative PAO navigation.

Jäger et al. [4] presented a study treating patients with a triple osteotomy, using a CT based navigation application. There was however no statistical evaluation of accuracy of acetabular reorientation. Langlotz et al. [5] reported on a first CT-based navigation application for PAO. This pioneer application offered visualization of the periacetabular cutting planes and assisted the surgeon during reorientation of the acetabulum and was applied to 14 clinical cases. However the application did not allow for pre-operative planning of the procedure and the surgeon could not refer to standard parameters defining acetabular orientation. Armand et al. [6] developed a computer-assisted Biomechanical Guidance System (BGS) for performing PAO. The system combines geometric and biomechanical feedback with intra-operative tracking to guide the surgeon through the PAO procedure.

However, Femoroacetabular impingement (FAI) before or after PAO surgery is surprisingly frequent and surgeons need to be aware of the risk and be able to avoid it [7]. Current computer-assisted planning and navigation is limited to PAO only and does not consider aspects of impingement. In this paper, for the first time we present a novel computer assisted planning and navigation system for PAO with range of motion (ROM) optimization. Details about our system are described below.

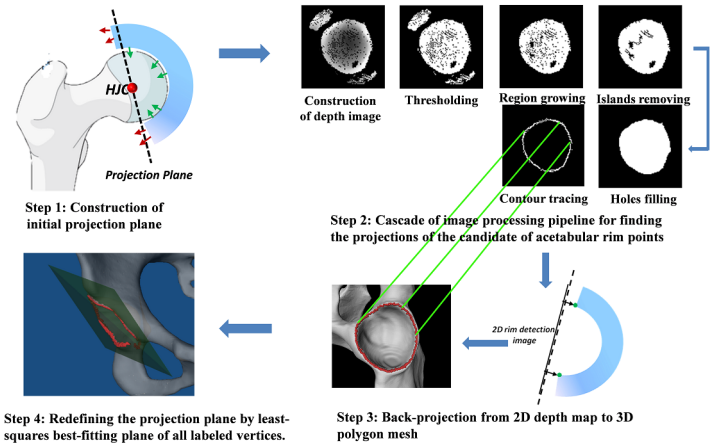

Fig. 2. Pipeline of fully automated acetabular rim detection

2 Materials and Methods

2.1 Workflow

The workflow of the developed system is shown in Fig. 1. It works in two stages: pre-operative planning stage and intra-operative navigation stage. The input to the pre-operative planning stage is 3D surface models of pelvis and femur generated from pre-operatively acquired CT data using a commercially available segmentation program (AMIRA, Visage Imaging, San Diego, USA). Two different local coordinate systems are then established using anatomical landmarks extracted from the CT data (see Fig. 1). One is defined for the pelvis on the anterior pelvic plane (APP) using the bilateral anterior superior iliac spines (ASISs) and the bilateral pubic tubercles [8], and the other is defined for the femur according to Murphy et al. [9] using the posterior condyles, the knee center and the femoral head center. After local coordinate systems are established, a fully automatic detection of the acetabular rim is conducted. The detected acetabular rims allow for automatically quantifying the acetabular morphology with parameters such as version, inclination and acetabular coverage. After that, virtual acetabular fragment reorientation simulation with hip impingement analysis is performed until an optimal ROM is obtained. The results from the planning stage are then passed to the intra-operative navigation stage where a visual feedback is provided during the acetabular fragment reorientation procedure in order to achieve the planned situation.

2.2 Fully Automated Acetabular Rim Detection

The acquisition of actebular rim is the prerequisite for quantifying hip joint morphology. We developed an improved algorithm of the rim detection method

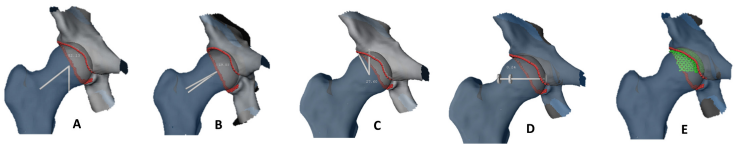

Fig. 3. Computing hip morphological parameters. (A) Acetabular Inclination; (B) Acetabular Anteversion; (C) Lateral Center Edge Angle (LCE); (D) Extrusion Index (EI); (E) Acetabular Coverage (AC).

originally introduced by Puls et al. [10]. In our method, the automated rim detection is achieved with the help of an acetabular projection plane, as shown in Fig. 2, which is initially constructed as a plane passing the femoral head center with a standard inclination of 45^o and anteversion of 20^o with respect to the local coordinate system of the APP. After that, following procedures are iteratively executed until convergence to automatically extract all acetabular rim points.

- Step 1: All vertices of the polygon mesh of pelvic model satisfying the following two criteria are projected onto the projection plane:
  - The distance between the vertices and the femoral head center are less than a predefined radius (in all our experiments, we set it to 7cm).
  - Normal vectors are oriented in the direction of the femoral head center.

  These criteria guarantee that only intra-articular vertices or some extra-articular vertices having a similar curvature as the acetabulum are projected.
- Step 2: A depth image is constructed out of the Euclidean distances between the vertices and the projection plane. A cascade of image processing pipeline is then developed to remove the extra-articular projection points and to find the 2D projections of the potential acetabular rim points, which are defined as the edges extracted from the 2D processed depth image (See Fig. 2).
- Step 3: 3D positions of these potential acetabular rim points are obtained by finding the corresponding 3D vertices of these 2D projections.
- Step 4: The projection plane is redefined via a least-squares fitting of all the potential acetabular rim points that we find so far.

The whole process is repeated until the normal vectors of two consecutively computed projection planes converge (angle difference $\leqslant 1.0^o$). The labeled vertices from the last iteration are defined as the resultant acetabular rim points.

2.3 Quantifying Hip Morphology

Accurate assessment of acetabular morphology and its relationship to the femoral head is essential for PAO planning. After acetabular rim points are extracted, least-squares fitting is used to fit a plane to these points. The fitted plane then allows for computing acetabular inclination (Fig. 3(A)) and anteversion (Fig. 3(B)) [11]. Additional hip morphological parameters such as the 3D Lateral Center Edge (LCE) angle (Fig. 3(C)), the 3D Extrusion Index (EI)(Fig. 3(D)),

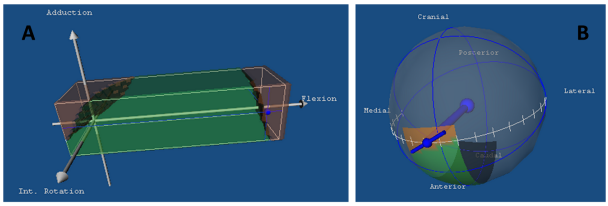

Fig. 4. ROM result visualization. (A): Visualization with Motion Box. The green areas represent impingement-free hip motions, whereas the brown areas refer to hip motions provoking impingement; (B): Visualization with Motion Sphere. The femur is represented by a cylinder. Orange areas on the surface of the sphere visualize femoral positions causing impingement. Green areas display impingement-free motion steps.

and the 3D Acetabular Coverage (AC)(Fig. 3(E)) are computed as well. LCE is depicted as an angle formed by a line parallel to the longitudinal pelvic axis and by the line connecting the center of the femoral head with the lateral edge of the acetabulum according to Wiberg [12]. EI is defined as the percentage of uncovered femoral head in comparison to the total horizontal head diameter according to Murphy et al. [13]. AC is defined to be a ratio between the area of the upper femoral head surface covered by the acetabulum and the area of the complete upper femoral head surface.

2.4 PAO Planning with Range of Motion (ROM) Simulation

The aim of ROM simulation is to enable the surgeon to accurately detect impingement areas and analyze the patients hip ROM after virtual reorientation procedure [14]. In the developed system, impingement analysis consists of three consecutive steps: the definition of the hip ROM to be analyzed, the impingement detection for the whole defined ROM, and the visualization of the computed results. In the first step, the hip ROM to be analyzed has to be defined by determining the maximal extension/flexion, adduction/abduction, and internal/external rotation. Based on these values, a motion path is computed including all possible combinations of motion parameters within the predefined motion ranges. In a subsequent impingement detection step, the hip joint is brought in every position of the motion path and possible impingement areas are detected with the help of the collision detection algorithm introduced by Gottschalk et al. [15].

After the detection of collisions, the analysis of the hip ROM is visualized with two different 3D graphs. A so-called Motion Box visualizes the results of the impingement analysis of the whole ROM (see Fig. 4(A)). This graph clearly presents the patient specific impingement-free motion of a hip joint as well as hip motions causing bony impingement in a graphical overview whose axes are defined as follows: the x-axis represents flexion and extension, the y-axis adduction and abduction, and z-axis displays internal and external rotation [16]. It means each position in the Motion Box represents a motion position with specific tri-axial combination. However, the analysis of this graph is rather challenging due to its

Table 1. Mean distance(mm) and standard deviation(STD:mm) between the rim points extracted with the present method and the interactive manual picking method

	Ace1	Ace2	Ace3	Ace4	Ace5	Ace6	Ace7	Ace8	Ace9	Ace10
Mean	1.1	0.8	0.7	0.8	0.7	0.8	0.7	0.7	0.7	0.7
STD	0.7	0.5	0.4	0.5	0.4	0.6	0.4	0.4	0.4	0.4

Table 2. The difference between actabular morphology parameters from the computed and manual picked acetabular rim

	Inclination (^{o})	Anteversion (^{o})	Acetabular Coverage (%)
Error	1.04 ± 0.95	0.6 ± 0.41	1.54 ± 1.31
p-value	$0.69 > 0.05$	$0.92 > 0.05$	$0.97 > 0.05$

multiple dimensionalities and therefore requires some experience for interpretation. Therefore a so-called Motion Sphere was used to represent the impingement results in a more intuitive manner (see Fig. 4(B)). In this graph, the femur is represented as cylinder ending in a sphere which symbolizes the rotation center. The result of the impingement analysis is visualized as a color-coded map on the surface of a sphere.

2.5 Experiment Design and Results

In order to validate our comprehensive PAO planning and navigation with range of motion optimization, three experiments were designed and conducted.

The purpose of the first experiment is to validate the accuracy and reliability of the automated acetabular rim detection. In total 10 computer assisted PAO procedures were performed on 5 cadavers (each cadaver has two hip joints). Three different methods were used to extract the rim points from each acetabulum: the automated rim detection method as presented in this paper, the method introduced by Puls et al. [10], and an interactive manual picking method, whose results are regarded as the ground truth. When our method was compared with the ground truth, mean distances were less than 1mm in 9 out of 10 cases (see Table 1), which is regarded accurate enough from a clinical point of view. When our method was compared with the method introduced by Puls et al. [10], our method generated much less rim points than theirs (on average 246 ± 29 points with our method vs. 1216 ± 153 points with their method) but with an accuracy similar to theirs. With less rim points detected, the simulation speed is improved.

For further validation purpose, we also compared hip morphological parameters computed from the extracted rim points. With a paired Student t-test, no statistically significant difference was found (see Table 2 for details).

The second experiment is designed to evaluate efficacy of two different PAO planning strategies. In total 10 computer-assisted PAO planning was performed on 7 real patients with acetabular dysplasia (AC: $62.4 \pm 6.5\%$). The first planning

Table 3. The improved ROM ratio (%) between Plan1 (without ROM optimization) and Plan2 (with ROM optimization)

	AC (%)	ROM (%)	ΔROM (%)	p-value
Plan 1	80.7 ± 5.6	71.0 ± 6.2	10.9 ± 3.1	1E-6 < 0.05
Plan 2	72.8 ± 5.3	81.9 ± 4.4		

Table 4. The error difference (^{o}) of decomposed motion components between pre-operative planning and intra-operative navigation situations

Error(^{o})	Ext Rot/Int Rot	Abd/Add	Ext/Flex
	0.7 ± 0.4	0.6 ± 0.4	0.9 ± 1.0

strategy is to reorient the acetabular fragment without taking hip impingement into consideration. The other planning strategy is to reorient the acetabular fragment with ROM optimization. It means that the reoriented pelvic model has to be stored for ROM analysis. The above-described Motion Box visualizes the results of the impingement analysis of the whole ROM consisting of impingement and impingement-free areas. We computed the ratio of impingement-free areas in Motion Box and investigated whether ROM improved significantly using the planning strategy with ROM optimization (see Table 3). It was found that ROM ratio obtained from the second planning strategy was increased by $10.9 \pm 3.1\%$ when comparing to that obtained from the first planning strategy. A statistically significant difference was found with a paired Student t-test (see Table 3 for details where p-value for ROM ratio < 0.05).

The third experiment is designed to verify the hypothesis that the pre-operative planned situation can be achieved intra-operatively with reasonable accuracy. In total 8 computer assisted PAO procedures was performed on 4 cadavers, on which pre-operative PAO planning with ROM optimization was conducted first. Subsequently the intra-operative navigation module was used to track acetabular and pelvic fragments, supporting and guiding the surgeon during the osteotomies around the acetabulum until the pre-operative plan was achieved. In order to assess the difference between the pre-operatively planned situation and the intra-operatively achieved result, we compared the decomposed rotation components derived from the acetabular fragment reorientation between the planned and intra-operative situations. The results are shown in Table 4. From this table, it can be seen that the average errors along three motion components (External Rotation/ Internal Rotation, Abduction/Adduction and Extension/Flexion) are $0.7^\circ \pm 0.4^\circ$, $0.6^\circ \pm 0.4^\circ$ and $0.9^\circ \pm 1.0^\circ$, respectively.

3 Discussions and Conclusions

In this paper, we presented a comprehensive planning and navigation system for PAO with ROM optimization. Our experimental results demonstrated that a

better preoperative assessment of impingement-free motion and the identification of impingement location help surgeon to optimally plan PAO surgery.

References

1. Ganz, R., Klaue, K., Vinh, T., Mast, J.: A New Periacetabular Osteotomy for the Treatment of Hip Dysplasia. Technique and Preliminary Results. Clin. Orthop. 232, 26–36 (1988)
2. Crockaress Jr., J., Trousdale, R.T., Cabanela, M.E., Berry, D.J.: Early Experience and Results with the Periacetabular Osteotomy. The Mayo Clinic experience. Clin. Orthop. 363, 45–53 (1999)
3. Rodriguez, A.C., Buckley, J.M., Diab, M., Burch, S.: An Evaluation of the Accuracy of Computer Assisted Surgery in Preoperatively Three Dimensionally Planned Periacetabular Osteotomies. In: 56th Annual Meeting of the Orthopaedic Research Society (2009)
4. Jager, M., Westhoff, B., Wild, A., Krauspe, R.: Computer-assisted Periacetabular Triple Osteotomy for Treatment of Dysplasia of the Hip. Z. Orthop. Ihre Grenzgeb 142, 51–59 (2004)
5. Langlotz, F., Bachler, R., Berlemann, U., Nolte, L.P., Ganz, R.: Computer Assistance for Pelvic Osteotomies. Clin. Orthop. 354, 92–102 (1998)
6. Armand, M., Lepisto, J.V.S., Merkle, A.C., Tallroth, K., Liu, X., Taylor, R.H., Wenz, J.: Computer-aided Orthopedic Surgery with Near-real-time Biomechanical Feedback. Johns Hopkins APL Technical Digest 25, 242–252 (2004)
7. Ziebarth, K., Balakumar, J., Domayer, S., Kim, Y.J., Millis, M.B.: Bernese Periacetabular Osteotomy in Males: Is There An Increased Risk of Femoroacetabular Impingement (FAI) after Bernese Periacetabular Osteotomy? Clin. Orthop. 469, 447–453 (2011)
8. Zheng, G., Marx, A., Langlotz, U., Widmer, K.H., Buttaro, M., Nolte, L.P.: A Hybrid CT–free Navigation System for Total Hip Arthroplasty. Computer Aided Surgery 7, 129–145 (2002)
9. Murphy, S.B., Simon, S.R., Kijewski, P.K., Wilkinson, R.H., Griscom, N.T.: Femoral Anteversion. J. Bone Joint Surg. Am. 69, 1169–1176 (1987)
10. Puls, M., Ecker, T.M., Steppacher, S.D., Tannast, M., Siebenrock, K.A., Kowal, J.H.: Automated Detection of the Acetabular Rim Using Three-dimensional Models of the Pelvis. Comput. Biol. Med. 41, 285–291 (2011)
11. Murray, D.W.: The Definition and Measurement of Acetabular Orientation. J. Bone Joint Surg. Br. 75(B), 228–232 (1993)
12. Wiberg, G.: The Anatomy and Roentgenographic Appearance of A Normal Hip Joint. Acta Chir. Scand. Suppl. 83, 7–38 (1939)
13. Murphy, S.B., Ganz, R., Muller, M.E.: The Prognosis in Untreated Dysplasia of the Hip. A Study of Radiographic Factors that Predict the Outcome. J. Bone Joint Surg. Am. 77, 985–989 (1995)
14. Tannast, M., Kubiak-Langer, M., Langlotz, F., Puls, M., Murphy, S.B., Siebenrock, K.A.: Noninvasive Three-dimensional Assessment of Femoroacetabular Impingement. J. Orthop. Res. 25, 122–131 (2007)
15. Gottschalk, S., Lin, M.C., Manocha, D.: Obbtree: A Hierachical Structure for Rapid Interference Detection. In: Rushmeier, H. (ed.) Proceedings of SIGGRAPH 1996, pp. 1169–1176. Addison Wesley (1996)
16. Thornberry, R.L., Hogan, A.J.: The Combined Use of Simulation and Navigation to Demonstrate Hip kinematics. J. Bone Joint Surg. Am. 91, 144–152 (2009)